The current issue and full text archive of this journal is available on Emerald Insight at:
https://www.emerald.com/insight/2755-0907.htm

Received 28 May 2024
Revised 3 July 2024
Accepted 5 July 2024

Research and design of an expert diagnosis system for rail vehicle driven by data mechanism models

Lin Li
Zhuzhou Guochuang Rail Technology Company Limited, Zhuzhou, China, and
Jiushan Wang and Shilu Xiao
Zhuzhou Guochuang Rail Technology Company Limited, Industrial Intelligence Research Institute, Zhuzhou, China

Abstract

Purpose – The aim of this work is to research and design an expert diagnosis system for rail vehicle driven by data mechanism models.

Design/methodology/approach – The expert diagnosis system utilizes statistical and deep learning methods to model the real-time status and historical data features of rail vehicle. Based on data mechanism models, it predicts the lifespan of key components, evaluates the health status of the vehicle and achieves intelligent monitoring and diagnosis of rail vehicle.

Findings – The actual operation effect of this system shows that it has improved the intelligent level of the rail vehicle monitoring system, which helps operators to monitor the operation of vehicle online, predict potential risks and faults of vehicle and ensure the smooth and safe operation of vehicle.

Originality/value – This system improves the efficiency of rail vehicle operation, scheduling and maintenance through intelligent monitoring and diagnosis of rail vehicle.

Keywords Rail transit, Rail vehicle, Expert diagnosis, Intelligent operation and maintenance, Deep learning, Lifespan prediction, Reliability analysis

Paper type Research paper

1. Introduction

With the continuous development of the Chinese economy, the rail transit industry in China is developing rapidly. In 2023, Chinese rail transit ridership once again set a record, with a daily average ridership exceeding 80 million people (Hou, Feng, Yan, & Zuo, 2024). At present, rail transit becomes the primary choice for public transportation in China. With the continuous growth of rail ridership, the number of operating vehicles increases, the operation time prolonging, the maintenance frequency increases and the difficulty of managing the entire lifecycle of vehicle and components increases. Therefore, traditional maintenance methods can no longer meet the increasingly complex operational needs. The introduction of intelligent operation and maintenance system brings new changes to rail transit operation and maintenance. Through sensing and IoT technology, real-time monitoring of vehicle status is achieved, ensuring the safety of vehicle operation and ride comfort.

© Lin Li, Jiushan Wang and Shilu Xiao. Published in *Railway Sciences*. Published by Emerald Publishing Limited. This article is published under the Creative Commons Attribution (CC BY 4.0) licence. Anyone may reproduce, distribute, translate and create derivative works of this article (for both commercial and non-commercial purposes), subject to full attribution to the original publication and authors. The full terms of this licence may be seen at http://creativecommons.org/licences/by/4.0/legalcode

This work was supported by Hunan Province Enterprise Technology Innovation and Entrepreneurship Team Support Program Project, Hunan Province Science and Technology Innovation Leading Talent Project [2023RC1088] and Hunan Province Science and Technology Talent Support Project [2023TJ-Z10].

Railway Sciences
Vol. 3 No. 4, 2024
pp. 480-502
Emerald Publishing Limited
e-ISSN: 2755-0915
p-ISSN: 2755-0907
DOI 10.1108/RS-05-2024-0016

Based on statistics and deep learning techniques, driven by state data, trend data and historical data, the system can predict the remaining lifespan of components and expose potential faults of components. Through real-time updating of maintenance information and automatic allocation of maintenance resources, the system will ensure timely maintenance for vehicle.

In recent years, intelligent operation and maintenance system receives increasing attention from researchers. A literature (Li, Lu, Wu, & Yang, 2023; Li, Xia, Hua, Wang, & Yao, 2023) analyzes and elaborates the framework and functions of vehicle intelligent operation and maintenance system, proposing to evaluate fault levels and hazards based on reliability, but there is no in-depth analysis of reliability calculation methods. A literature (Hu, 2019) introduces a rail transit intelligent operation and maintenance system that has been put into operation in Shanghai. In this system, machine vision, sensing and deep learning technology is used to automatically monitor key components such as pantographs, wheels and brake shoes without stopping. The literature also illustrates the engineering significance brought by these technologies. However, this literature does not deeply analyze the mechanism of the deep learning monitoring model. A literature (Cai, Gao, Meng, Xuan, & Zhong, 2023) proposes the development of standard interface protocols to address issues such as diverse vehicle equipment manufacturers, diverse component types and incompatible interface protocols, enabling the system to collect data more comprehensively. However, traditional data collection equipment requires wiring and installation of power supplies, and the position of the equipment is difficult to adjust in the later stage. A literature (Lv, 2021) establishes a health assessment model and a lifespan prediction model for key components of vehicle running gear. Driven by state data, trend data and historical data, the health level of key components of running gear is evaluated, and the lifespan is predicted, thereby carrying out preventive maintenance and generating considerable economic benefits, demonstrating the engineering significance. A literature (Aida, Dnislam, Aruzhan, Daniil, & Dimitrios, 2024) proposes using IoT technology to monitor the location of vehicle in real-time, sending out warnings to nearby personnel, avoiding safety accidents.

In order to solve the problems existing in current intelligent operation and maintenance system, this work researches and designs an expert diagnosis system for rail vehicle based on data mechanism model driving. Time series analysis is a classic statistical method processes data which changes over time to predict the occurrence time of future faults. Based on this method, specific calculation rules based on relevant theories and experiences is designed. According to these rules, the system can automatically calculate reliability score (Pan, 2021) of vehicle and subsystems, and then identifies potential problems that may cause the fault of the vehicle or subsystems in advance. In addition, deep learning technology develops rapidly, this type of technology relies on a large amount of historical and similar data to train component fault diagnosis models and then uses state data to drive the model to achieve online diagnosis (Tu, Zhang, & Wang, 2020). The data-driven intelligent operation and maintenance system cannot do without data acquisition technology. Wireless passive sensing technology is an emerging data acquisition technology (Li, Lu, *et al.*, 2023; Li, Xia, *et al.*, 2023). Compared to traditional data acquisition devices, wireless passive acquisition devices do not require cables and power, have stronger environmental adaptability and are more convenient to install and have lower costs. Therefore, wireless passive sensing technology is more suitable for data collection in intelligent operation and maintenance system.

2. System architecture research and design

Due to the limitations of vehicle structure, the expert diagnostic system is divided into two parts: onboard and ground. The original vehicle data is transmitted to the onboard system

(Jiang *et al.*, 2018) through Multifunctional Vehicle Bus (MVB), subsequently, relying on wireless transmission devices and Ethernet, the onboard system transmits historical and current data to the ground system. Finally, utilize statistical and deep learning methods, drive the data mechanism models with vehicle historical data, current data and similar data to achieve intelligent monitoring and diagnosis for rail vehicle. The architecture design of the Expert Diagnosis System is shown in Figure 1.

As shown in Figure 1, the Expert Diagnosis System consists of reliability analysis, operation analysis, operation monitoring, subsystems and vehicle resume management. (1) The reliability analysis module is used to evaluate the ability of the vehicle and subsystems to achieve their expected functions within a certain time or mileage, including the vehicle MTBF, vehicle MDBF, subsystem MDBF and overall evaluation. The specific implementation details are arranged in section 3.1 of the paper. (2) The operation analysis module includes lifespan prediction, energy consumption analysis and fault trend analysis. Through lifespan prediction, operators can implement preventive maintenance measures according to the remaining lifespan of components. To predict the probability and time nodes of fault occurrence more accurately and estimate the remaining lifespan of vehicle components more accurately, deep learning idea is introduced in this work. The core idea of deep learning is to train predictive models using labeled data (Liu, Jin, & Wang, 2023; Susanne, Thorsten, Gerrit, Arnout, & Douwe, 2024). Specifically, the first step is to collect raw data through MVB. Then, clean the original data, including filling in omissions, eliminating anomalies and smoothing out noise. Next, use data dimensionality reduction, feature extraction and feature fusion to obtain the feature matrix. Subsequently, the pre-trained model which has already been initialized is trained through the training set, and the model is improved to address any existing issues. Finally, validate the performance of the model using the validation set. If the verification is successful, the model will be put into the expert diagnosis system. Through energy consumption analysis, operators can identify high energy consuming areas and take corresponding measures to reduce energy consumption. Through fault trend analysis, operators can identify subsystems with more potential faults. The specific implementation details of operational analysis are arranged in section 3.2 of the paper. (3) The operation monitoring module is responsible for online monitoring and analysis of all vehicles operating on the line, including line monitoring, status preview, vehicle monitoring, HMI synchronization and fault monitoring. The specific implementation details are arranged in section 3.3 of the paper. (4) The vehicle is dividing into multiple subsystems according to their functions, including traction, battery, braking, air-conditioning, vehicle door, smoke and fire subsystems. The system monitors and diagnoses the critical states of the

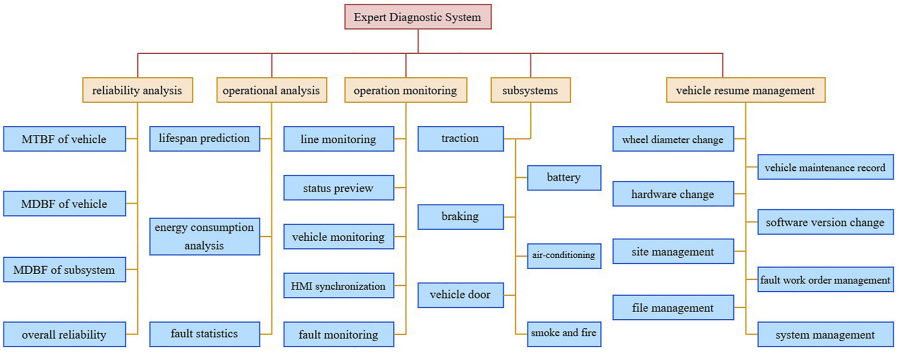

Figure 1.
Architecture design of the expert diagnosis system

Source(s): Authors' own work

subsystems, and the specific implementation details are arranged in section 3.4 of the paper. (5) The vehicle resumes management module mainly records hardware changes, vehicle maintenance, software version changes and other information. It also has functions such as site management, file management and system management. The specific implementation details are arranged in section 3.5 of the paper.

The efficient and stable operation of the system cannot be separated from hardware support. On the ground, the main hardware facilities include expert diagnostic system servers, pantograph monitoring servers, running gear monitoring servers, dispatch room terminals, technical room terminals, network switches and photoelectric converters. The minimum power required by the system is 26kVA (meet the 60 minutes power supply demand).

3. System function research and design

3.1 Reliability analysis

Reliability analysis is a system engineering method. It is used to evaluate the ability of a vehicle and subsystems to achieve its expected functions, within a certain period. This analysis aims to identify and solve problems, which may cause the failure of the vehicle or subsystems. Also, this analysis aims to provide guidance to improve the reliability and safety of the vehicle. Reliability analysis can be divided into four parts: Mean Time Between Failures (MTBF) of vehicle, Mean Distance Between System Failures (MDBF) of vehicle, MDBF of subsystem and overall reliability.

(1) MTBF of vehicle

MTBF of vehicle refers to the elapsed time that the expected vehicle fault occurs under normal operating conditions, usually expressed in hours. The higher the value, the better the reliability. Calculate the MTBF at the end of each day of vehicle operation. The reliability grading method for the MTBF of vehicle is as follows:

- Obtain the number of historical vehicle faults N before the end of operation time. Obtain the historical running time T_N of the vehicle before the end of operation time.
- Calculate the $SCORE_{MTBF}^{vehicle}$ at the end of operation: $SCORE_{MTBF}^{vehicle} = \frac{T_N}{N}$.
- Table 1 is the MTBF reliability grading table for vehicle. MTBF of vehicle can be graded according to the calculated $SCORE_{MTBF}^{vehicle}$ and the grading rules in Table 1.

(2) MDBF of vehicle

MDBF of vehicle refers to the elapsed mileage that the expected vehicle fault occurs under normal operating conditions, usually expressed in kilometer. The higher the value, the better the reliability. Calculate MDBF once after a certain operating cycle. The reliability grading method for the MDBF of vehicle is as follows:

Rank	MTBF/h	SCORE
1	>220	10
2	[200, 220]	9
3	[180, 200)	6
4	<180	4

Source(s): Authors' own work

Table 1. MTBF of vehicle grading table

- Obtain the number N of historical failures at the end of operation. Obtain the vehicle mileage M_N at the end of operation.
- Calculate the $SCORE^{vehicle}_{MDBF}$ at the end of operation: $SCORE^{vehicle}_{MDBF} = \frac{M_N}{N}$.
- Table 2 is the MDBF of vehicle reliability grading table. The MDBF of vehicle can be graded according to the calculated $SCORE^{vehicle}_{MDBF}$ and the grading rules in Table 2.

(3) MDBF of subsystem

Calculate MDBF of subsystem at the end of each day of vehicle operation. The reliability grading method for the MDBF of subsystem is as follows:

- Obtain the number N^i of operational failures for each subsystem at end of operation, where i represents the sequence of subsystem. Obtain vehicle mileage M_N at end of operation.
- Calculate the $SCORE^i_{MDBF}$ of each subsystem at the end of operation: $SCORE^i_{MDBF} = \frac{M_N}{N^i}$.
- Table 3 is the MDBF of subsystem grading table. The MDBF of subsystem can be graded according to the calculated $MDBF$ and the grading rules in Table 3.

(4) Overall reliability

When evaluating the overall reliability of a vehicle, it is necessary to comprehensively consider each subsystem, and this step adopts a deduction algorithm. The total deduction value D of the subsystems can be expressed as follows:

$$D = \sum_{i=1}^{N} SCORE^i \times 10 \tag{1}$$

Table 2. MDBF of vehicle grading table

Rank	MDBF/km	SCORE
1	>200000	10
2	[180000, 200000]	9
3	[160000, 180000)	6
4	<160000	4

Source(s): Authors' own work

Table 3. MDBF of subsystem grading table

Subsystem	MTBF/km	$SCORE^i$
Traction	1800000	0.2
Braking	1020000	0.2
Running gear	15000000	0.2
Pantograph	4620000	0.1
Vehicle door	1020000	0.1
Air-conditioning	2340000	0.1
Auxiliary	1800000	0.1

Source(s): Authors' own work

where, N denotes the total number of subsystems, $SCORE^i$ is the score of the i-th subsystem. $SCORE^i$ is shown in Table 3. D is not allowed to exceed 5.

The overall reliability evaluation score S of the vehicle is represented as follows:

$$S = SCORE_{MTBF}^{vehicle} \cdot 0.35 + SCORE_{MDBF}^{vehicle} \cdot 0.65 - D \quad (2)$$

Obviously, the larger the S value, the higher the overall reliability of the vehicle.

Figure 2(a) shows the MDBF of each vehicle on a monthly basis. The score is obtained by taking the average daily score. Among them, the horizontal axis represents the vehicle number, and the vertical axis represents the score. According to the calculation rules, the higher the MDBF, the higher the failure rate of the vehicle. Therefore, special attention should be paid to the fault situation of vehicles numbered "503", "518", "520", "504", "515".

Figure 2(b) shows the MDBF of each subsystem on a daily basis, the horizontal axis represents the date, the vertical axis represents the score. The MDBF of Train Running Department System (TDS) is the highest and more resources should be input into investigating the TDS.

3.2 Operation analysis

3.2.1 Lifespan prediction. Predicting the lifespan of vehicle components can detect potential faults and damages in advance, implement preventive maintenance measures and minimize downtime and maintenance costs caused by sudden failures. The lifespan prediction model is driven by data mechanism, which collects historical data, similar component data and degradation data of components. This model predicts the lifespan of components based on statistical, degradation, reliability functions and deep learning methods. As shown in Figure 3, data mechanism-driven lifespan prediction models can be divided into three categories according to different types of input data: degradation models, similarity models and survival models.

(1) Degradation model: This type of model requires obtaining degradation experimental data of the target component, such as the degradation curve of the health index. Linear models, exponential models and ARMA models can be used to fit the degradation curves. In addition, deep learning methods can be used for training to obtain the degradation model of the target component. After obtaining the degradation curve or degradation model, the lifespan of component can be predicting. (2) Similar model: This type of model relies on the

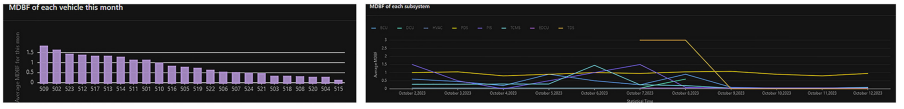

(a) (b)

Source(s): Authors' own work

Figure 2.
MDBF score of each vehicle and subsystem

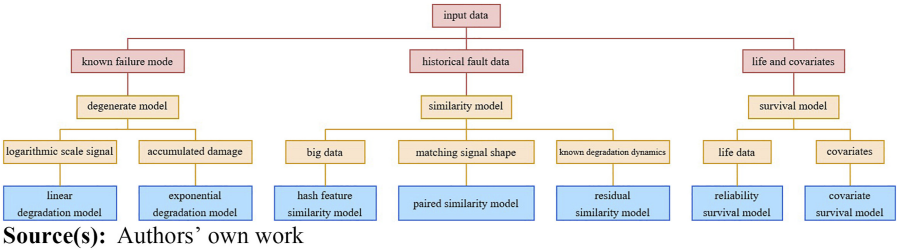

Source(s): Authors' own work

Figure 3.
Data-driven lifespan prediction models

historical lifespan data of similar components, which should reflect a degradation trend from normal working state to failure state. (3) Survival model: If the historical data of similar components only includes lifespan data and covariates, without degradation data, a survival model should be used for prediction. This model only focuses on the distribution of component lifespan, such as mean, standard deviation and variance. In addition, covariates refer to environmental variables or explanatory variables, which can be the manufacturing batch, manufacturer, etc. of the component.

Long Short-Term Memory (LSTM) is a typical temporal feature neural network model and a type of degraded model (Sepp & Jürgen, 1997). LSTM includes forget gate, input gate and output gate. The function of forget gates is to forget unnecessary information, the function of input gates is to collect key information and the function of output gates is to output key information. This model is time sensitive and can retain distant contextual information when processing sequential data, learning temporal features in the data. Therefore, LSTM has significant advantages in the field of component lifespan prediction (Lu, Wang, Zhang, & Gu, 2024). LSTM mainly consists of three parts: input gate, forget gate and output gate. The mechanism model of LSTM can be represented as:

$$i_t = \sigma(\omega_i \cdot [h_{t-1}, x_t] + b_i) \tag{3}$$

$$\overline{C}_t = \tanh(\omega_t \cdot [h_{t-1}, x_t] + b_t) \tag{4}$$

$$f_t = \sigma(\omega_f \cdot [h_{t-1}, x_t] + b_f) \tag{5}$$

$$C_t = f_t \cdot C_{t-1} + i_t \cdot \overline{C}_t \tag{6}$$

$$o_t = \sigma(\omega_0 \cdot [h_{t-1}, x_t] + b_0) \tag{7}$$

$$h_t = o_t \cdot \tanh(C_t) \tag{8}$$

where, Equations (3~4) denote the input gate, i_t is the update weight of new features, σ is Sigmod activation function, ω_i and b_i is the weight and offset of the input gate, h_{t-1} is the output of the unit at previous moment, x_t is the current input, $\overline{C}_t$ is the updated candidate vector, tanh is Hyperbolic tangent activation function, ω_t and b_t is the current weight and offset. Equations (5~6) denote the forget gate, f_t is the chance of forgetting, ω_f and b_f is the weight and offset of the forget gate, C_t is the current state, C_{t-1} is the state at previous moment. The forget gate determines which unnecessary features to forget and retains useful features. Equations (7~8) denote the output gate, o_t is the output threshold, ω_0 and b_0 is the weight and offset of the output gate, h_t is the output of the current unit.

As shown in Figure 4, this work integrates vibration signals, current signals and bearing temperature characteristics, constructing a motor bearing lifespan prediction model based on LSTM and Attention Mechanism. Specifically, first of all, use Principal Component Analysis (PCA) to reduce the dimensionality of vibration signals, current signals and bearing

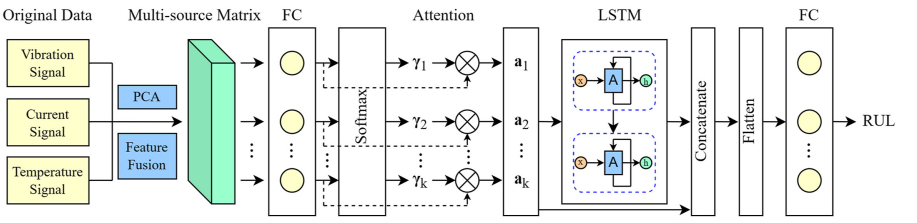

Figure 4.
A motor bearing lifespan prediction model based on LSTM and attention mechanism

Source(s): Authors' own work

temperatures. Next, extract features from the original data, and fuse them into a multi-source information feature matrix. Subsequently, the multi-source information feature matrix is transmitted to the Full Connection (FC) layer. Then, the scores are converted into probability distributions through the Softmax activation function. Next, the Attention layer enhances the core feature weights, the LSTM layer mines deep temporal features and then the Concatenate layer concatenates the attention layer with the LSTM output results. Finally, after processing with the Flatten layer and the FC layer, the Remaining Useful Lifespan (RUL) is output.

In the training phase, a low learning rate may lead to slow model convergence speed, while an excessively high learning rate may cause gradient explosion problems. An appropriate learning rate can quickly converge the model to the global minimum, reduce prediction errors and improve model performance. The learning rate is set to 0.002 in this work. Excessive LSTM layers may lead to over-fitting, weakening the model's generalization ability and too deep layers can increase training difficulties. The LSTM layers are set to 2 in this work.

In order to evaluate the predictive ability of the model, Mean Absolute Error (MAE) and Root Mean Squared Error (RMSE) is used to quantitatively analyze the prediction results. The calculation formulas for the above evaluation indicators are expressed as:

$$MAE = \frac{1}{m}\sum_{i=1}^{m}|y_i - \widehat{y}_i| \tag{9}$$

$$RMSE = \sqrt{\frac{1}{m}\sum_{i=1}^{m}(y_i - \widehat{y}_i)^2} \tag{10}$$

where, m is the number of samples, y_i is the true value, $\widehat{y}_i$ is the predicting value.

3.2.2 Energy consumption analysis. Energy consumption analysis aims to promote cost control and environmental protection. By analyzing energy consumption data, it is possible to identify the parts with higher energy consumption and take targeted measures to reduce energy consumption. By measuring energy consumption and implementing energy-saving measures, electricity consumption can be reduced, thereby reducing carbon emissions from thermal power generation. Energy consumption analysis mainly calculates the daily unit energy consumption, average unit energy consumption, recent unit energy consumption, recent unit energy consumption deviation, maximum deviation of this month and day-on-day ratio of unit energy consumption. The unit energy consumption on that day reflects the energy consumption status of the vehicle. If the energy consumption status is abnormal, further investigation is needed. The energy consumption data directly obtained from the vehicle is the cumulative value. Therefore, it is necessary to first obtain the cumulative energy consumption value, and then calculate the unit energy consumption for the day. Calculate the daily unit energy consumption of the vehicle at the end of the day's operation, use the following calculation method:

(1) Obtain the traction energy consumption at the beginning of the day's operation C_t^s, energy consumption of braking resistor C_b^s, regenerated energy E_r^s and load data L^s. Then, obtain the traction energy consumption at the end of the day's operation C_t^e, energy consumption of braking resistor C_b^e, regenerated energy E_r^e and load data L^e.

(2) Calculate the daily unit energy consumption of the vehicle f:

$$f = \frac{C_t^e - C_t^s + C_b^e - C_b^s - \left(E_r^e - E_r^s\right)}{L^e - L^s} \tag{11}$$

Figure 5 shows the real statistical results of energy consumption on a vehicle that has been put into operation. The changes in driving mode, braking strategy and ridership flow will significantly affect energy consumption. Different driving modes and braking strategies can lead to different energy consumption. By analyzing energy consumption, operators can adjust driving modes and braking strategies to save energy. And also, operators can speculate peak period of ridership by analyzing energy consumption.

3.2.3 Fault statistics. Fault trend analysis is beneficial for optimizing maintenance strategies, predicting maintenance needs and improving vehicle design. Figure 6 shows fault trend analysis of several subsystems, the frequency of faults occurring of bow net in August is relatively high, also the door control. Therefore, the operators should focus on the relevant data in August, investigate the reasons for the high incidence of faults and make corresponding improvements.

Comprehensive statistics are conducted on subsystem failures according by the timeline. This work focuses on analyzing subsystems with significant month-on-month growth, to identify systemic design defects and potential risks in vehicles and provide data support for improving vehicle design. As shown in Figure 7, the number of BCU (Battery Control Unit)

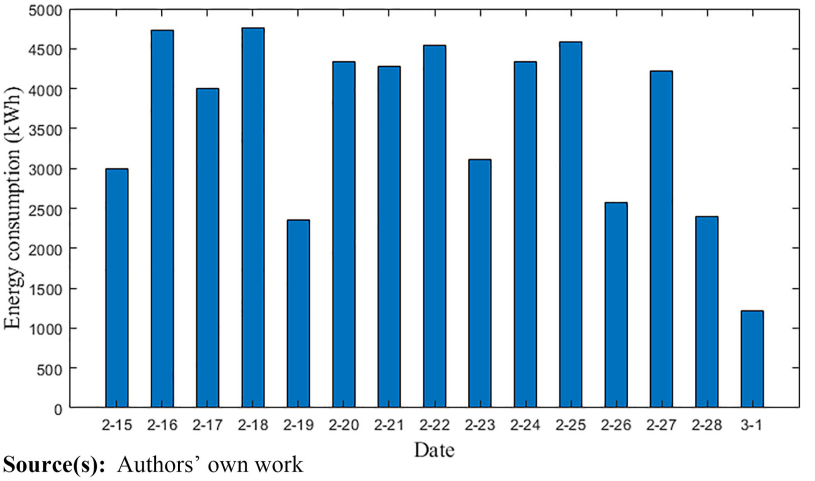

Source(s): Authors' own work

Figure 5.
Real statistical results of energy consumption

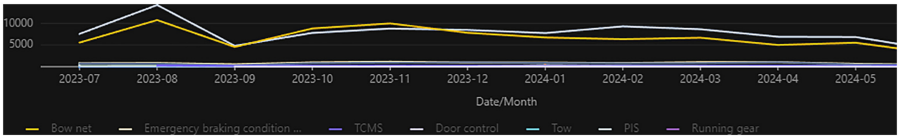

Figure 6.
Trend analysis of subsystem faults

Number	Subsystems	Number of faults	Fault percentage	Failure rate (this month)	Failure rate (last month)	Failure rate (same month last year)	YoY	Month on month ratio	Statistical time
1	BCU	80	0.567	0.567	0.536	0.67	84.671%	105.813%	2024-05-01
2	DCU	5	0.035	0.035	0.006	0	0%	621.65%	2024-05-01
3	EDCU	1	0.007	0.007	0.034	0.012	57.153%	20.722%	2024-05-01
4	HVAC	5	0.035	0.035	0	0	0%	0%	2024-05-01

Source(s): Authors' own work

Figure 7.
Comprehensive statistics of subsystem faults

subsystem faults significantly increases. Therefore, the operators should conduct a fault investigation on this subsystem.

3.3 Operation monitoring

Operation monitoring is the online monitoring and analysis of all vehicles on the line. The system includes five items: line monitoring, status preview, vehicle monitoring, HMI synchronization and fault monitoring. The core monitoring sub items and purposes of the operation monitoring system are shown in Table 4.

(1) Monitor vehicle driving speed

To monitor the vehicle driving speed, it is necessary to use a traction motor speed measurement system to measure the traction motor speed. The core component of the traction motor speed measurement system is the Hall element. The main working principle of the Hall element is the Hall effect: when a conductor crosses a magnetic field, free electrons will be subjected to the Lorentz force, causing electrons to produce lateral displacement inside the conductor, resulting in positive charge accumulation on one side of the conductor and negative charge accumulation on the other side, ultimately generating voltage horizontally on the conductor. At the non-transmission end of the traction motor, the standard involute magnetic speed measuring gear rotates coaxially with the motor rotor and the measurement system can sense voltage pulse signals related to speed through the Hall effect. After the motor speed is measured, the vehicle driving speed can be calculated. The traction motor speed measurement system is shown in Figure 8.

As shown in Figure 8, the traction motor speed measurement system mainly consists of EMC/EMI circuit, Hall element, threshold detection element, driver, push-pull and permanent

Item	Sub item	Purpose
Line monitoring	line overview	Monitor the distribution of online and offline vehicles on the line, provide a basis for optimizing scheduling
	vehicle driving status	Monitor vehicle mileage and direction of travel, provide a basis for vehicle maintenance and scheduling
	line fault	Collect and display line fault information, identify vehicle colors based on severity level
Status preview	vehicle status	Display vehicle information in three states: main line, in warehouse and offline
Vehicle monitoring	vehicle speed	Monitor speed through traction motor speed measurement gear
	traction energy consumption	Monitor changes in energy consumption, provide data support for cost analysis and control
	fire alarm and fire extinguisher status	Prevent fires and initiating fire alarms
HMI synchronization	pantograph status	Determine if the pantograph is abnormal, monitoring network voltage and network flow
	carbon contact strip warning	Implement carbon contact strip warning based on historical wear data and current mileage
	Battery pack status	Monitor the voltage, current and temperature of the battery pack
Fault statistics	fault statistics	Statistics faults comprehensively in various systems include power distribution system, monitoring information viewing system, door control unit, brake control unit

Source(s): Authors' own work

Table 4. The core monitoring sub items and purposes of the operation monitoring system

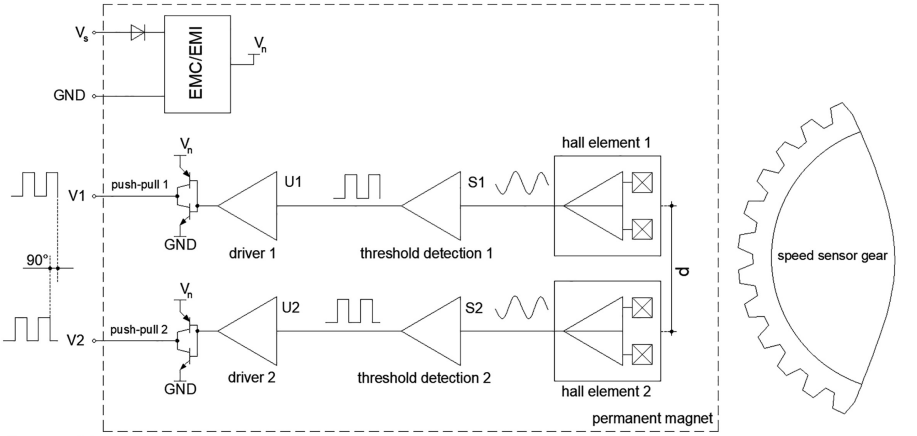

Source(s): Authors' own work

Figure 8.
Traction motor speed measurement system

magnet. When the speed measuring gear on the right is working, the tooth valley and tooth bottom alternate across the permanent magnet, forming a regular magnetic field change on the surface of the permanent magnet. After the two Hall elements sense the magnetic field change, they convert the magnetic field change into voltage signals S1 and S2. After receiving S1 and S2, the threshold detection element converts them into square waves U1 and U2. Finally, the square waves pass through the push-pull circuit to form standard square waves V1 and V2. By manually controlling the spacing d between Hall elements, the phase deviation between V1 and V2 can be reduced to 90°, with one being a sine wave and the other being a cosine wave. Finally, based on V1 and V2, the output pulse frequency f of the speed sensor can be calculated. Due to the calculation of output pulses by comparing the output signals of two Hall elements, it can effectively counteract external temperature changes, electromagnetic interference and other disturbances, making the traction motor speed measurement system have higher measurement accuracy in complex environments. After obtaining the output pulse frequency f of the speed sensor, the vehicle driving speed v can be calculated:

$$\begin{cases} v_r = \dfrac{60f}{n} \\ v = iv_r \pi D_w \end{cases} \tag{12}$$

where, v_r (*r/min*) is the speed of the traction motor, f is the output pulse frequency of the speed sensor, n is the number of teeth of the speed measuring gear, i is the transmission ratio of the power system, D_w (m) is the wheel diameter.

(2) Recognize abnormal state of pantograph intelligently

As a key component of the power system, the status of the pantograph has a significant impact on the smooth and safe operation of the vehicle. Severe faults in the pantograph during operation may cause interruptions in vehicle operation and even lead to safety accidents. Therefore, during the operation of the vehicle, it is necessary to timely monitor the structural damage, spark splashing and other abnormal states of the pantograph. Manual monitoring requires labor costs and cannot avoid observation errors caused by long-term continuous work. Therefore, camera equipment can be used to capture pantograph images,

and computer vision technology intelligent recognition technology can be introduced to achieve automated and intelligent monitoring of abnormal pantograph conditions (Song, Wang, & Ren, 2023). In the field of computer vision image recognition, VGG (Karen & Andrew, 2014) is a mainstream convolutional neural network model. VGG adopts a relatively regular stacking of convolutional and pooling layers, organizing them into modular block structures. Each block uses the same convolutional kernel size and step size internally, making the network structure clearer and easier to adjust and optimize parameters. Given the above advantages, on the basis of VGG model, use pantograph images as driving data to achieve intelligent recognition of abnormal pantograph states. The intelligent recognition model for abnormal status of pantographs based on VGG is shown in Figure 9.

The working mechanism of the intelligent recognition model for abnormal status of pantographs based on VGG is as follows. Firstly, scale the pantograph image uniformly to a size of $224 \times 224 \times 3$ and input it into the first convolutional layer of the VGG model. Place 3×3 convolutional kernels in the convolutional layer and combine every three kernels into one convolutional sequence to construct a wider receptive field. Then, place 2×2 pooling cores in the pooling layer and extract the main features using pooling processing. After 13 rounds of convolution and five rounds of pooling processing, advanced features are mapped to the corresponding label space through 4096, 4096 and 1000 sized Fully Connected layers in sequence. Finally, normalization is performed using the Softmax function to obtain the category probability, which is used to determine whether the pantograph status is abnormal.

During the training phase, a cross-entropy loss function is used to train the intelligent recognition model for pantographs. The loss function of this model can be expressed as:

$$Loss = -\frac{1}{N}\sum_{t=1}^{N}[r(x_t)\ln(p(x_t)) + (1 - r(x_t))\ln(1 - p(x_t))] \tag{13}$$

where, $Loss$ is the difference between the predicted value and the actual value in each iteration, N is the number of samples, x_t is the t-th sample, $r(x_t)$ is the actual label of the t-th sample, $p(x_t)$ is the predicted output of the t-th sample. After the model reached convergence state through training, samples were extracted from the pantograph test set for validation. After verification, put the model into the operational environment.

The pantograph images in the dataset are captured from the pantograph monitoring videos of multiple vehicles. In order to obtain more features under different working

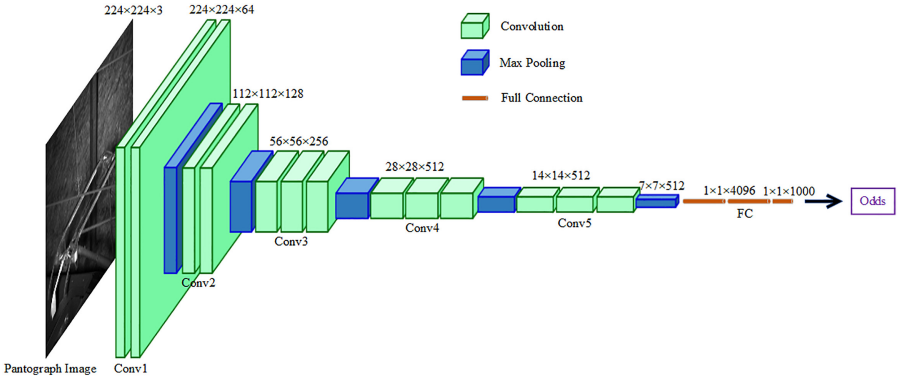

Source(s): Authors' own work

Figure 9. Intelligent recognition model for abnormal status of pantographs based on VGG

conditions, environmental factors such as lighting, rain and snow, indoor and outdoor conditions are fully considered when capturing images. In addition, using random translation, random rotation, random flipping, random scaling and random color transformation to generate new images on the original image enhances data diversity. In most images, the pantograph is located at the center, and the pantograph area accounts for approximately 15% of the entire image. The size of the original image is $640 \times 640 \times 3$, which is inconsistent with the input size of the model. Therefore, interpolation method is used to adjust the size of the image to $224 \times 224 \times 3$.

Use accuracy and recall rate to evaluate the performance of the model. Normal pantograph images are considered positive samples, and abnormal pantograph images are considered negative samples. Accuracy refers to the ratio of the number of correctly classified samples to the total number of samples. The correct classification of both positive and negative samples is counted. As the purpose of this work is to identify abnormal pantographs, the recall rate is set to the negative samples. Specifically, the negative sample recall rate refers to the proportion of samples correctly identified as negative samples among all actual negative samples.

(3) Carbon contact strip early warning algorithm

Due to the long-term high strength working conditions of the pantograph carbon contact strip, it often bears enormous pressure and friction, making it prone to wear and failure. To ensure the smooth and safe operation of vehicle, it is necessary to implement early warning algorithm for carbon contact strip. On the premise that the carbon contact strip and working environment have not undergone significant changes, due to the similarity between similar components, the historical replacement data of carbon contact strip has high reference value. Therefore, statistical methods can be used to calculate the high-risk range of current collection mileage $[m_{min}, m_{max}]$ from historical replacement data. The carbon contact strip early warning algorithm is shown in Figure 10.

3.4 Subsystem

3.4.1 Traction subsystem.

(1) Online fault diagnosis for traction inverter IGBT

The vehicle obtains direct current from the overhead contact system through the pantograph, and then the direct current is transmitted to the traction inverter. The traction inverter

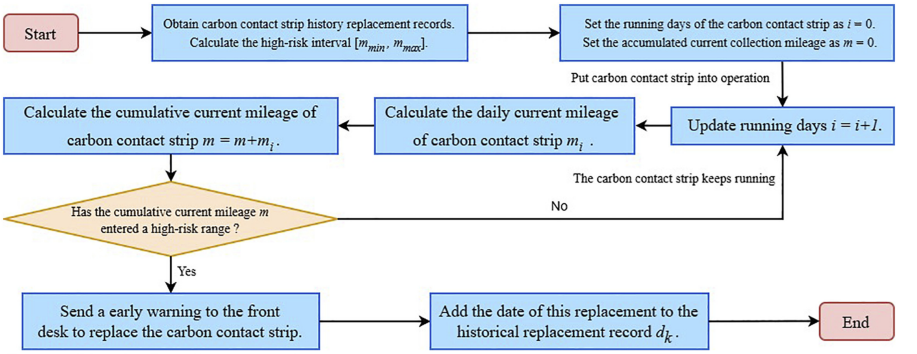

Figure 10.
Carbon contact strip early warning algorithm

Source(s): Authors' own work

regulates direct current and converts it into three-phase alternating current, thereby driving three-phase asynchronous AC traction motors and achieving traction. During vehicle operation, the traction inverter is a high-risk area of faults, with Insulated Gate Bipolar Transistor (IGBT) faults occurring most frequently (Liu, 2018). IGBT faults can be divided into short circuit faults and open circuit faults. Short circuit faults can cause a rapid increase in current, but most inverters are integrated with detection circuits, which immediately cut off the IGBT after a short circuit fault occurs, thereby transforming the short circuit fault into an open circuit fault. A single IGBT open circuit fault will not immediately have a significant negative impact, but it will cause an imbalance in the stator current of the traction motor, causing motor torque fluctuations and a decrease in motor speed (Jia, 2023), affecting the normal operation of the vehicle. Therefore, online fault diagnosis of traction inverter IGBT is of great significance.

In the traction inverter circuit, an IGBT open circuit fault can cause a loss of current in some circuits, resulting in distortion of the output current signal. The principle of an open circuit fault in a single IGBT of the traction inverter is shown in Figure 11. If an open circuit fault occurs in IGBT tube S_1 on the A-phase circuit, the current i_A will rapidly decay to 0 within half a cycle, causing distortion of the inverter output current. Although the distorted current signal can reflect the presence of faults in the inverter, it is difficult to accurately analyze the location of the fault directly through the current signal. Therefore, it is necessary to introduce a signal filtering method to extract fault feature vectors from distorted current signals and establish a relationship model between each fault feature vector and each real IGBT fault, to achieve accurate positioning of IGBT faults. Furthermore, considering the high computational speed requirement for online diagnosis, the diagnostic process needs to minimize delays as much as possible. Therefore, a high-speed filtering method should be adopted. Considering the above factors, the Wavelet transform method is introduced to extract feature vectors from distorted currents.

Wavelet transform (Minesh and Patel, 2024) is an improved version of Fourier transform, which can not only extract target feature vectors from complex raw current signals, but also has the advantage of fast solving speed, making it suitable for online diagnosis of traction inverter IGBT. According to different application fields, wavelet transform can be divided into discrete wavelet transform and continuous wavelet transform. The output

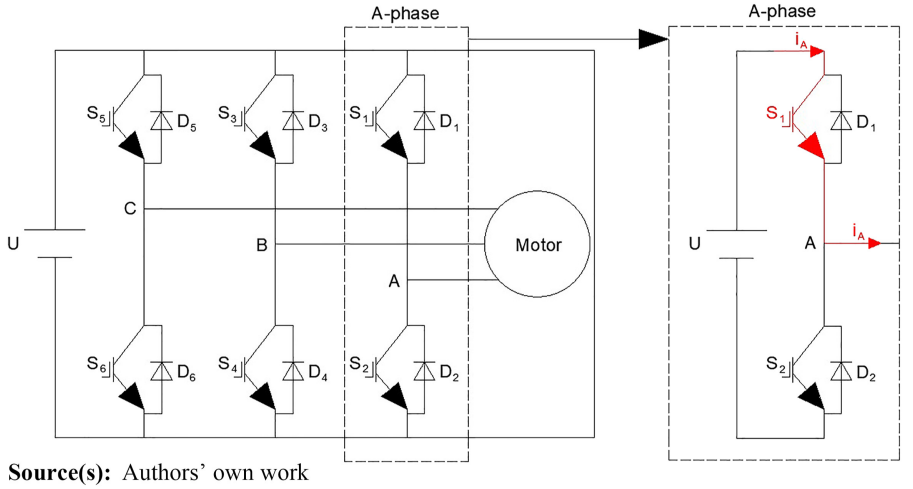

Source(s): Authors' own work

Figure 11.
An open circuit fault in a single IGBT of the traction inverter

current of the inverter is a continuous signal, therefore continuous wavelet transform is adopted. Continuous wavelet transform can extract different frequency components of continuous signals. Then, the feature vectors related to IGBT faults will be obtained from the components. The principle of continuous wavelet transform can be expressed as:

$$W(a,b) = \int_{-\infty}^{\infty} f(t) \frac{1}{\sqrt{a}} \Psi\left(\frac{t-b}{a}\right) dt \tag{14}$$

where, $W(a,b)$ is the result of continuous wavelet transform, a is a scale factor, b is a translation factor, $f(t)$ is an input current signal, $\Psi\left(\frac{t-b}{a}\right)$ is the mother wavelet function. When the scale factor a is large, the wavelet function is pulled up, making it easier to analyze low-frequency signals. When the scale factor b is small, the wavelet function is squeezed, making it easier to analyze high-frequency signals. Therefore, the input signal can be decomposed into low-frequency and high-frequency signals through continuous wavelet transform.

The working principle of online fault diagnosis for traction inverter IGBT based on wavelet transform is as follows. Firstly, collect the output current signal of the inverter and transmit it to the expert diagnostic system. Next, initialize the mother wavelet function based on existing engineering experience. Next, perform continuous wavelet transform on the output current signal of the inverter to obtain low-frequency signals. Next, extract feature vectors from low-frequency signals. Next, determine the IGBT fault location based on the existing IGBT fault location-feature vector relationship model. Finally, send the IGBT fault information to the front desk and issue a fault alarm message.

(2) Monitor transmission shaft torque

In the traction subsystem, the torque of the transmission shaft is an important component of measuring the traction performance of the vehicle. Also, the torque of the transmission shaft is an important basis for judging whether the transmission shaft is working properly and whether it is in the optimal working condition. The surface acoustic wave torque sensor deployed on the surface of the transmission shaft is a wireless and passive torque sensor. Compared with traditional torque sensors, surface acoustic wave torque sensors have the advantages of using wireless communication technology to transmit data, no wiring required, less susceptible to interference, no need for external power supply, flexible layout, small size and low cost. Surface acoustic wave torque sensors are made of piezoelectric materials. When an electric field is applied to a piezoelectric crystal, the piezoelectric effect causes the crystal to vibrate, forming a surface acoustic wave. When the piezoelectric substrate (usually quartz) on the sensor is subjected to external stress changes, the external strain deviation can cause changes in the parameters of the piezoelectric material (Khalfi *et al.*, 2023), further altering the resonant frequency of the resonator.

When the transmission shaft is not subjected to torque, the resonant frequency f_0 of the resonator can be expressed as:

$$f_0 = \frac{v_0}{\lambda} = \frac{v_0}{4a_0} \tag{15}$$

where, v_0 is the propagation velocity of surface acoustic waves on the surface of piezoelectric substrates, λ is the wavelength of surface acoustic waves, a_0 is the distance between the electrodes. When the transmission shaft is subjected to torque, strain is generated. The propagation speed of surface acoustic waves on piezoelectric substrates changes, the electrode spacing also changes, the above two cause a change in resonant frequency. At this point, the resonant frequency $f(\varepsilon)$ can be represented as:

$$f(\varepsilon) = \frac{v_0(1+\alpha\varepsilon)}{4a_0(1+\varepsilon)} = f_0\frac{1+\alpha\varepsilon}{1+\varepsilon} \tag{16}$$

where, α is the constant of the piezoelectric substrate material. For the surface strain of the shaft ε, its magnitude is generally 10^{-3}, and at this time, the strain of the piezoelectric substrate is approximately linearly related to the resonant frequency of the surface acoustic wave resonator. Finally, the torque M of the transmission shaft can be expressed as:

$$M = \frac{\pi E D^3 \Delta f}{16(1+\mu)kf_0} \tag{17}$$

where, E is the strain tensor on the surface of the piezoelectric substrate, D is the diameter of the transmission shaft, Δf is the frequency change of the resonator after disturbance, μ is the displacement under disturbance, k is the strain sensitivity of the acoustic surface wave and f_0 is the resonant frequency without strain disturbance.

The single ended resonant surface acoustic wave torque sensor (Wang, Yao, & Li, 2022) has certain shortcomings. This is because in actual working environments, high-speed rotating torque sensors are affected by harsh environments such as electromagnetic fields and temperature, leading to measurement errors. In order to reduce the impact of adverse environmental factors on torque detection and improve the sensitivity of torque detection, two surface acoustic wave resonators with similar performance sensitive to corresponding variable parameters are often used to form a differential measurement structure for torque measurement. The basic scheme of a torque monitoring system based on surface acoustic wave torque sensors is shown in Figure 12. When the system operates, the sensor antenna emits excitation, the reader antenna receives the sensor signal and transmits the signal to the reader module for analysis, thereby calculating the shaft torque.

(3) Monitor the temperature of traction motor

During vehicle operation, if the temperature of the traction motor exceeds the warning value, it is likely to cause motor failure, resulting in power attenuation or loss and serious safety issues. Therefore, in order to monitor the motor temperature in real time, a Pt100 four-wire temperature monitoring system was installed at all four traction motor stators of the vehicle. Pt100, also known as 100 ohms platinum resistance, is used because platinum materials have the characteristics of corrosion resistance, oxidation resistance, high sensitivity and high temperature resistance. The above advantages making Pt100 suitable for working in harsh

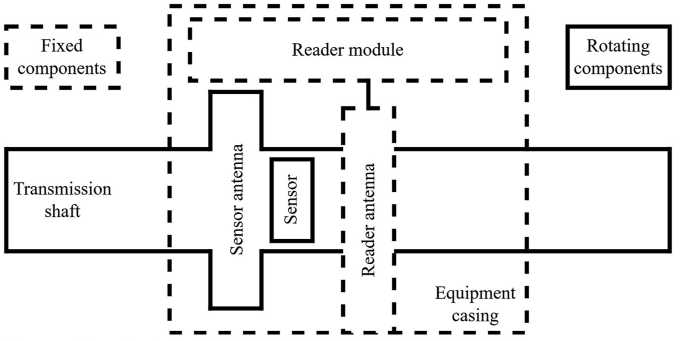

Source(s): Authors' own work

Figure 12.
A basic scheme of torque monitoring system

environments of traction motors in rail vehicle (Wang, 2019). The temperature measurement range of the Pt100 temperature sensor is −200~850 °C, the normal working temperature of traction motor is generally not lower than −60 °C and not higher than 200 °C, which meets the temperature measurement requirements. The relationship between the resistance of platinum resistance and ambient temperature within the range of −200~850 °C can be expressed as:

$$R_t = \begin{cases} R_0\left(1 + At + Bt^2 + C(t-100)t^3\right), & -200℃ \le t \le 0℃ \\ R_0\left(1 + At + Bt^2\right), & 0℃ \le t \le 850℃ \end{cases} \tag{18}$$

where, R_t (Ω) is the resistance value of a platinum resistor at temperature t, and R_0 (Ω) is the resistance value of a platinum resistor at 0°C. The temperature measurement resistor used in this work is Pt100 type, therefore $R_0 = 100\Omega$. A、B and C is the Pt100 resistance coefficient value, $A = 3.9082 \times 10^{-3}$, $B = -5.80195 \times 10^{-3}$, $C = -4.2735 \times 10^{-3}$.

The two-wire circuit connection method is the most basic platinum resistance temperature measurement method, but in this method, the presence of lead resistance will reduce the temperature measurement accuracy. In contrast, the four-wire temperature measurement circuit is almost unaffected by lead resistance, thus achieving high-precision measurement.

Figure 13 shows the Pt100 four-wire temperature measurement circuit. Where, I_s is a constant current source, Pt100 is the temperature measurement resistor, R_1、R_2、R_3、R_4 are the resistors of four leads and the amplifier on the right is a differential amplifier. As analyzed earlier, the presence of leads R_3 and R_4 will interfere with the measurement of the voltage U_p at both ends of Pt100. To solve the above problem, a high impedance differential amplifier is connected in series with R_3 and R_4, so that the current passing through R_3 and R_4 is infinitely close to 0. Therefore, $U_p = U_d$. This design basically eliminates the interference of lead resistance on the temperature measurement circuit.

Set the differential amplification factor to k, there is $U_e = kU_d = kU_p$. Use a voltmeter to measure U_e, combine Equation (18), the relationship between the working temperature t of the traction motor and the temperature measurement resistance R_t can be expressed as:

$$R_t = \frac{U_p}{I_s} = \frac{U_e}{kI_s} = R_0\left(1 + At + Bt^2 + C(t-100)t^3\right), \quad -200℃ \le t \le 0℃ \tag{19}$$

$$R_t = \frac{U_p}{I_s} = \frac{U_e}{kI_s} = R_0\left(1 + At + Bt^2\right), \quad 0℃ \le t \le 850℃ \tag{20}$$

Table 5 is the Pt100 graduation table of the traction motor.

Table 5 shows the resistance of the Pt100 temperature measurement resistor of the traction motor at different temperatures. Through this table, the approximate current temperature of the traction motor can be quickly queried.

3.4.2 Battery pack monitoring system. The battery pack monitoring system of the expert diagnostic system aims to monitor and diagnose the voltage, current and temperature. In the event of a power outage or malfunction in the power grid, the battery pack serves as a backup

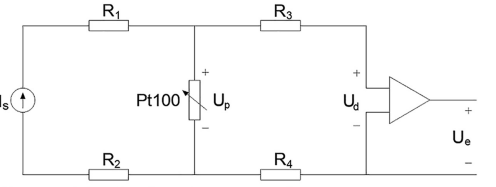

Source(s): Authors' own work

Figure 13.
Pt100 four-wire temperature measurement circuit

power source to provide power to the power system, communication system and door system, to maintain normal vehicle operation. To ensure the normal power supply of the battery pack, it is necessary to monitor the above status. For this purpose, a battery pack monitoring system was constructed and the system structure is shown in Figure 14.

As shown in Figure 14, voltage and current sensors are installed on each battery cell to monitor the voltage of each cell. At the same time, the total voltage of the entire battery pack is monitored through the total voltage measurement circuit, and the current is monitored through the current measurement circuit. In addition, install one temperature sensor on each battery unit to monitor the temperature of each unit. Finally, the above monitoring data are transmitted to the expert diagnostic system through the battery pack management system. After analysis and diagnosis, the diagnostic results are displayed on the front end of the expert diagnostic system.

3.4.3 Braking subsystem. According to the source of braking force, vehicle braking modes can be divided into two types: electric braking and pneumatic braking. According to braking requirements, the braking modes of vehicles in motion can be divided into service braking, rapid braking and emergency braking. Due to the large inertia of rail vehicles, precise braking is difficult and the braking performance of vehicles is closely related to safety, online monitoring of vehicle braking systems is crucial. The working principle of the online brake monitoring system is shown in Figure 15.

The braking force sources for both service braking and rapid braking are the same, using a hybrid power system that combines electric and pneumatic braking. The main difference between the two is that the deceleration of rapid braking is greater than that of service braking, which can achieve faster braking. Electric braking is generally used at high speeds. When the electric brake is triggered, the motor is converted into a generator, converting

Temperature (℃)	0	+5	+10	+15	+20	+25	+30	+35	+40	+45
	Resistance value(Ω)									
−50	80.31	82.29	84.27	86.25	88.22	90.19	92.16	94.12	96.09	98.04
0	100.00	101.95	103.90	105.85	107.79	109.73	111.67	113.61	115.54	117.47
50	119.40	121.32	123.24	125.16	127.08	128.99	130.90	132.80	134.71	136.61
100	138.51	140.40	142.29	144.18	146.07	147.95	149.83	151.71	153.58	155.46
150	157.33	159.19	161.05	162.91	164.77	166.63	168.48	170.33	172.17	174.02
200	175.86	177.69	179.53	181.36	183.19	185.01	186.84	188.66	190.47	192.29

Source(s): Authors' own work

Table 5.
Pt100 graduation table of the traction motor

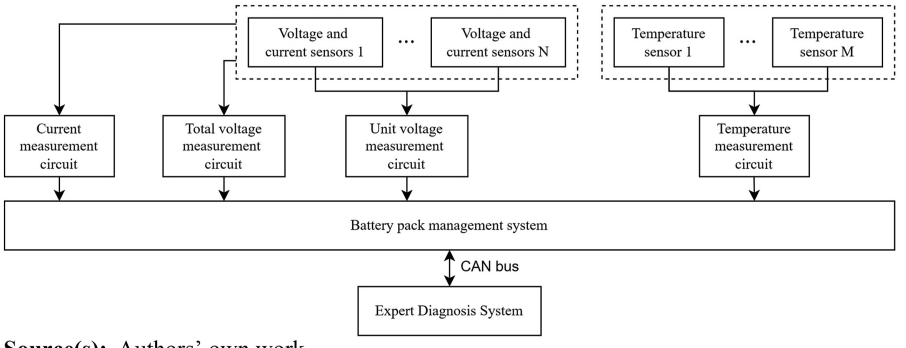

Source(s): Authors' own work

Figure 14.
Battery pack monitoring system

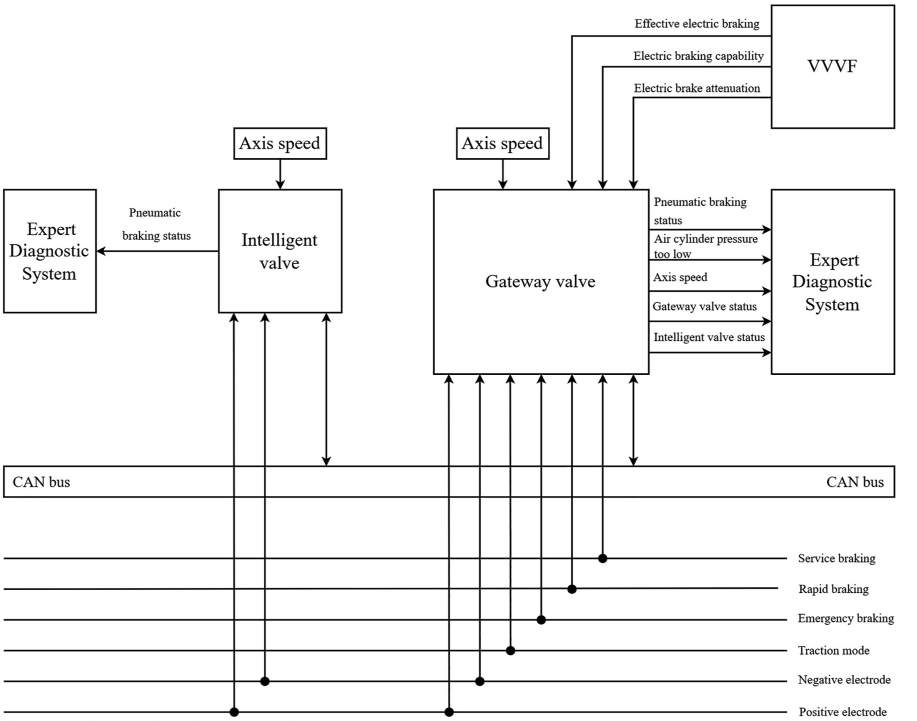

Source(s): Authors' own work

Figure 15.
Online brake monitoring system

kinetic energy into electrical energy, generating a counter torque to prevent the vehicle from moving forward. When the vehicle speed drops to the threshold, pneumatic braking begins to intervene. At this time, electric braking and pneumatic braking work simultaneously, ultimately achieving the vehicle's parking. As shown in Figure 15, Variable Voltage and Variable Frequency (VVVF) is a variable frequency speed control system used to control traction motors. When the electric braking starts, VVVF sends an effective electric braking signal and actual electric braking force to the gateway valve. However, as the electric brake is activated, the vehicle speed will continue to decrease, resulting in a continuous attenuation of the electric braking force. When the electric braking force decays to the threshold, VVVF will send an electric braking attenuation signal to the gateway valve. During the entire braking process involving electric braking, the gateway valve will transmit the effective electric braking signal, actual electric braking force and electric braking attenuation signal to the expert diagnostic system. The above data will be displayed on the monitoring interface after being diagnosed by the expert diagnostic system, as shown in Figure 16. The diagnostic

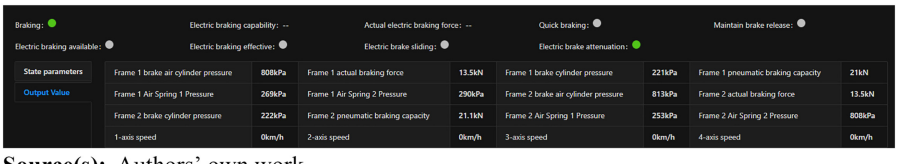

Source(s): Authors' own work

Figure 16.
Key braking parameter monitoring interface

indicators include theoretical electric braking capacity, actual electric braking force, pneumatic braking capacity, brake cylinder pressure and axis speed.

Sometimes, there are fewer vehicles and power consuming components operating in the power grid, and the electrical energy generated through electric braking cannot be fully consumed by the power grid. At this time, the increase in network voltage may damage electronic components. To avoid the above situation, a braking resistor is introduced in the electric braking circuit. The main function of a braking resistor is to convert electrical energy into thermal energy, and then dissipate the thermal energy into the atmosphere through natural ventilation or forced ventilation. In actual operation, if the heat dissipation is not sufficient, it will cause the temperature of the braking resistor to be too high, causing the braking resistor to burn out and causing the vehicle to lose some of its electric braking capacity. For example, if the surface of the braking resistor cabinet is contaminated with soil, it will seriously reduce the heat dissipation performance. It can be seen that in order to ensure the electric braking capability of vehicles, online monitoring of brake resistance temperature is indispensable. When the temperature of the braking resistor exceeds the safety threshold, the expert diagnostic system will issue an alarm message to remind the staff to troubleshoot the problem.

Emergency braking is a braking mode used in emergency situations, which only uses pneumatic braking mode and can quickly generate maximum braking force and deceleration. The pneumatic braking system mainly consists of an air compressor, air cylinder, air duct, brake cylinder and brake shoe. Firstly, use an air compressor to compress the air and push the compressed air into the air cylinder. Subsequently, when the air brake command is issued, the compressed air in the air cylinder is transmitted to the brake cylinder through the air duct. Finally, the brake cylinder exhausts compressed air, pushing the brake shoe to contact the wheel tread, creating braking resistance. It can be seen that in the process of pneumatic braking, real-time monitoring of the changes in brake cylinder pressure and air cylinder pressure is crucial. Insufficient pressure may lead to brake failure, posing a safety hazard. As shown in Figure 15, the gateway valve collects data on pneumatic braking status, cylinder pressure and axis speed, while the intelligent valve only collects data on pneumatic braking status. Subsequently, the gateway valve and intelligent valve transmit the above data to the expert diagnostic system. Finally, the above data were diagnosed by an expert diagnostic system and displayed on the monitoring interface, as shown in Figure 16. The diagnostic indicators for pneumatic braking include brake cylinder pressure, actual braking force, air cylinder pressure and axis speed.

3.5 Vehicle resume management

Vehicle resume management includes vehicle maintenance records, wheel diameter changes, hardware changes, software version changes, site management, fault work order management, file management and system management. (1) Vehicle maintenance records: By recording the maintenance status and history of vehicles, it can ensure that they are regularly maintained and repaired, reducing safety hazards caused by failure to detect and repair problems in a timely manner. Meanwhile, through maintenance records, product quality issues and production process defects can be identified and manufacturer could take measures to improve product quality. In the vehicle maintenance record module, the maintenance vehicle, the system to which the maintenance part belongs, the fault name, fault level, maintenance time, warranty personnel and detailed operation information will be recorded. (2) Wheel diameter change: As the track is divided into standard gauge, narrow gauge and wide gauge, different wheel diameters are required to adapt to the track. The expert diagnostic system will capture and record the changes in the wheel diameter value of the carriage, forming a wheel diameter change record, which includes the latest wheel

diameter value, wheel diameter update time and historical change records. (3) Hardware change: When making changes to the vehicle's hardware, the change information will be retained in the hardware change module. The change information includes vehicle number, hardware name, model and specifications, material code, manufacturer and serial number. (4) Software version changes: In actual development work, due to frequent changes in business requirements and adjustments in business logic, version iteration and replacement are relatively frequent. To ensure the traceability of code, software version management is essential. Recording software version changes can track the software's change history, including modification content, modification time and modifier information, which helps to understand the software's development process, trace the root cause of problems and evaluate improvements and changes between different versions. If necessary, software can be rolled back based on the old version. The content of the software version change module includes line number, vehicle number, software name, software version and software time. (5) Site management: In the site management module, staffs can create new sites, modify site information and delete sites. The site information includes the route it belongs to, the site ID and the site name. (6) Fault Work Order Management: In order to achieve more efficient management, a complete maintenance information chain has been designed for fault work orders. The maintenance information includes work order number, fault occurring time, fault vehicle number, subsystem name, repair personnel, maintenance task personnel, current fault status, fault start and end time, specific fault description and fault review personnel. Through the fault work order management module, both repair personnel and maintenance personnel can view and maintain fault information in the fault work order system, reducing communication costs in daily operations and improving operational efficiency. (7) File Management: The file management module mainly manages technical files and message logs. Technical documents, technical data and message log files sent by onboard subsystems are centrally managed here, providing functions such as retrieval, download and preview. (8) System Management: In the system management module, staffs can create, edit and delete user account and query existing user information.

4. Conclusion

This expert diagnostic system has been officially put into operation. This system mainly achieves following functions: Through the reliability analysis of the vehicle and subsystems, identifies and solves system failure problems in advance; Predicts the remaining lifespan of key components based on LSTM and Attention Mechanism model; Recognizes abnormal pantograph status intelligently based on VGG convolutional neural network model; Implements carbon contact strip early warning based on similarity algorithm; Monitors torque of transmission shaft accurately based on wireless passive surface acoustic wave torque sensor; Monitors traction motor operating temperature accurately based on Pt100 four-wire temperature measurement circuit; Collects relevant braking signals and diagnose the current braking status through an online brake monitoring system. After verification, it is found that the system can issue a warning within three seconds after the fault occurs, in other words, the corresponding time of the system does not exceed three seconds. Overall, this expert diagnosis system introduces artificial intelligence methods and precise online monitoring technology, provides an intelligent and high-precision monitoring and diagnosis system for urban rail transit operations. In the future, the next step of the work is to introduce digital twin technology on the basis of this system. Digital twin is a virtual mapping technology based on data and artificial intelligence for real-world objects, it can establish a digital copy of the vehicle. Next, through the digital model, staff can further diagnose the entire lifecycle of the vehicle and eliminate existing hidden faults in advance.

Reference

Aida, E., Dnislam, U., Aruzhan, S., Daniil, O., & Dimitrios, Z. (2024). Ad-hoc train-arrival notification system for railway safety in remote areas. *Internet of Things*, *25*, 101062. doi: 10.1016/J.IOT.2024.101062.

Cai, Y., Gao, F., Meng, Y., Xuan, X., & Zhong, J. (2023). Design of intelligent operation and maintenance system for urban rail transit equipment and study on its key technologies. *Railway Computer Application*, *32*(7), 79–83. doi: 10.3969/j.issn.1005-8451.2023.07.15.

Hou, X., Feng, C., Yan, H., & Zuo, C. (2024). Overview of urban rail transit operational lines in Chinese mainland in 2023. *Urban Rapid Rail Transit*, *37*(1), 10–16. doi: 10.3969/j.issn.1672-6073.2024.01.002.

Hu, J. (2019). Research and application of intelligent operation and maintenance system for Shanghai rail transit vehicles. *Modern Urban Transit*, *7*, 5–9.

Jia, J. (2023). Research on fault diagnosis of multiple units traction inverters based on wavelet analysis. *China Railway*, *8*, 117–125. doi: 10.19549/j.issn.1001-683x.2023.05.25.002.

Jiang, Y., Liu, H., Song, H., Kong, H., Wang, R., Guan, Y., & Sha, L. (2018). Safety-assured model-driven design of the multifunction vehicle Bus controller. *IEEE Transactions on Intelligent Transportation Systems*, *19*(10), 3320–3333. doi: 10.1109/tits.2017.2778077.

Karen, S., & Andrew, Z. (2014). Very deep convolutional networks for large-scale image recognition. *IEICE Transactions on Fundamentals of Electronics, Communications and Computer Sciences*, *1409*, 1556.

Khalfi, H., Naciri, I., Raghib, R., Randrianarivelo, J., Yu, J., Ratolojanahary, F., & Elmaimouni, L. (2023). Axisymmetric free vibration modeling of a functionally graded piezoelectric resonator by a double Legendre polynomial method. *Acta Mechanica*, *235*(2), 615–631. doi: 10.1007/S00707-023-03766-1.

Li, Z., Lu, Q., Wu, G., & Yang, H. (2023). Research on the construction of intelligent operation and maintenance system for subway vehicles. *Science and Technology & Innovatio*, *14*, 43–45+48.

Li, Q., Xia, H., Hua, H., Wang, Z., & Yao, W. (2023). Passive wireless vibration sensing and monitoring system for railway freight car bogies. *Rolling Stock*, *61*(1), 124–130. doi: 10.3969/j.issn.1002-7602.2023.01.026.

Liu, C. (2018). Common faults and maintenance of traction inverters for subway vehicles. *Science and Technology Innovation Herald*, *15*(19), 37+39. doi: 10.16660/j.cnki.1674-098X.2018.19.037.

Liu, C., Jin, J., & Wang, Y. (2023). Construction of an intelligent operation and maintenance system platform based on pre-trained large models. *Technology and Market*, *30*(9), 13–18.

Lu, W., Wang, Yu., Zhang, M., & Gu, J. (2024). Physics guided neural network: Remaining useful life prediction of rolling bearings using long short-term memory network through dynamic weighting of degradation process. *Engineering Applications of Artificial Intelligence*, *127*(B), 107350. doi: 10.1016/J.ENGAPPAI.2023.107350.

Lv, C. (2021). Health assessment and life prediction system for axle box bearing of urban rail transit vehicle running gear. *Urban Mass Transit*, *24*(S1), 149–153.

Minesh, K., & Patel, R. R. (2024). Fault detection through discrete wavelet transforms and radial basis function neural network in shunt compensated distribution systems. *Engineering Research Express*, *6*(2), 025335. doi: 10.1088/2631-8695/AD46E7.

Pan, Y. (2021). Fault statistics and reliability analysis of rail transit vehicles. *Journal of Shanghai Electric Technology*, *14*(3), 44–47.

Sepp, H., & Jürgen, S. (1997). Long short-term memory. *Neural Computation*, *9*(8), 1735–1780. doi: 10.1162/neco.1997.9.8.1735.

Song, G., Wang, G., & Ren, G. (2023). Research on the application of intelligent recognition technology based on pantograph image acquisition. *Railway Vehicles*, *61*(5), 143–148. doi: 10.3969/j.issn.1002-7602.2023.05.027.

Susanne, R., Thorsten, N., Gerrit, S., Arnout, V., & Douwe, B. (2024). Expert system based fault diagnosis for railway point machines. *Proceedings of the Institution of Mechanical Engineers, Part F: Journal of Rail and Rapid Transit*, *238*(02), 214–224. doi: 10.1177/09544097231195656.

Tu, X., Zhang, S., & Wang, M. (2020). Fault diagnosis methodology based on deep-confidence network traction motor bearing. *Urban Mass Transit*, *23*(1), 174–178+195. doi: 10.16037/j.1007-869x.2020.01.042.

Wang, X. (2019). Analysis of the principle and debugging method of Pt100 temperature sensor on locomotive. *Technology And Market*, *26*(5), 22–25.

Wang, H., Yao, M., & Li, L. (2022). Characteristic test of a sensitive core of silicon resonant pressure sensor. *Measurement & Control Technology*, *41*(9), 84–89. doi: 10.19708/j.ckjs.2022.02.212.

Corresponding author
Jiushan Wang can be contacted at: 954547617@qq.com

For instructions on how to order reprints of this article, please visit our website:
www.emeraldgrouppublishing.com/licensing/reprints.htm
Or contact us for further details: **permissions@emeraldinsight.com**